Supporting information

A quantitative study of chemical kinetics for the synthesis of doped oxide nanocrystals using FTIR spectroscopy

Na Zhang,[1,2†] Xin Wang,[1†] Zhizhen Ye[1] and Yizheng Jin,[1,3*]

[1] *State Key Laboratory of Silicon Materials, Cyrus Tang Center for Sensor Materials and Applications, Department of Materials Science and Engineering, Zhejiang University, Hangzhou 310027, People's Republic of China*

[2] *Department of Chemistry, Zhejiang University, Hangzhou 310027, People's Republic of China*

[3] *Center for Chemistry of High-Performance and Novel Materials, Zhejiang University, Hangzhou 310027, People's Republic of China*

Corresponding author: yizhengjin@zju.edu.cn (Dr. Yizheng Jin)

[†] *Both authors contributed equally to this work.*

1. Characterization techniques.

FTIR spectra were obtained with a Bruker Vector 27 spectrophotometer.

The UV-Vis absorption spectra were recorded using a Shimadzu UV 3600 spectrophotometer.

TEM observations were performed on a JEOL JEM 1230 or a Hitachi 7700 electron microscope operated at 80 keV.

HRTEM images were obtained using a FEI TECNAI F20 electron microscope operated at 200 keV.

ICP-AES analyses were carried out by using an IRIS Intrepid II XSP ICP-AES equipment. The samples were prepared by dissolving the purified oxide nanocrystals in concentrated nitric acid (75%).

Thermo gravimetric analysis (TGA) of the zinc precursors were carried out on a SDT Q600 Simultaneous analyzer. The samples were heated from room temperature to 600 ºC at a rate of 10 ºC/min under an air flow.

EDS mapping and high-angle annular dark-field (HAADF) measurements were carried out on a aberration-corrected scanning transmission electron microscope (FEI Titan Chemi-STEM) equipped with an in-built Bruker Super-X EDS detectors which is operated at 200kV. The probe current is set to about 100 pA, and the convergent angle is 21.4 mrad.

2. Preparation and characterization of the zinc precursors.

$Zn(My)_2$ and $Zn(De)_2$ were synthesized according to literature methods.[1,2] For the synthesis of $Zn(My)_2$**,** a methanol solution of HMy (20 mmol) was neutralized by a methanol solution containing TMAH (20 mmol). Next a methanol solution of $Zn(NO_3)_2 \cdot 6H_2O$ (10 mmol) was introduced into the neutralized solution by dropwise addition. A white precipitate formed immediately. The precipitates were washed by methanol three times and dried in a vacuum oven at 50 ºC. The synthetic procedures for $Zn(De)_2$ were identical to those for $Zn(My)_2$ except that HMy was replaced by HDe.

The zinc precursors were characterized by FTIR and TGA (Figure S1).

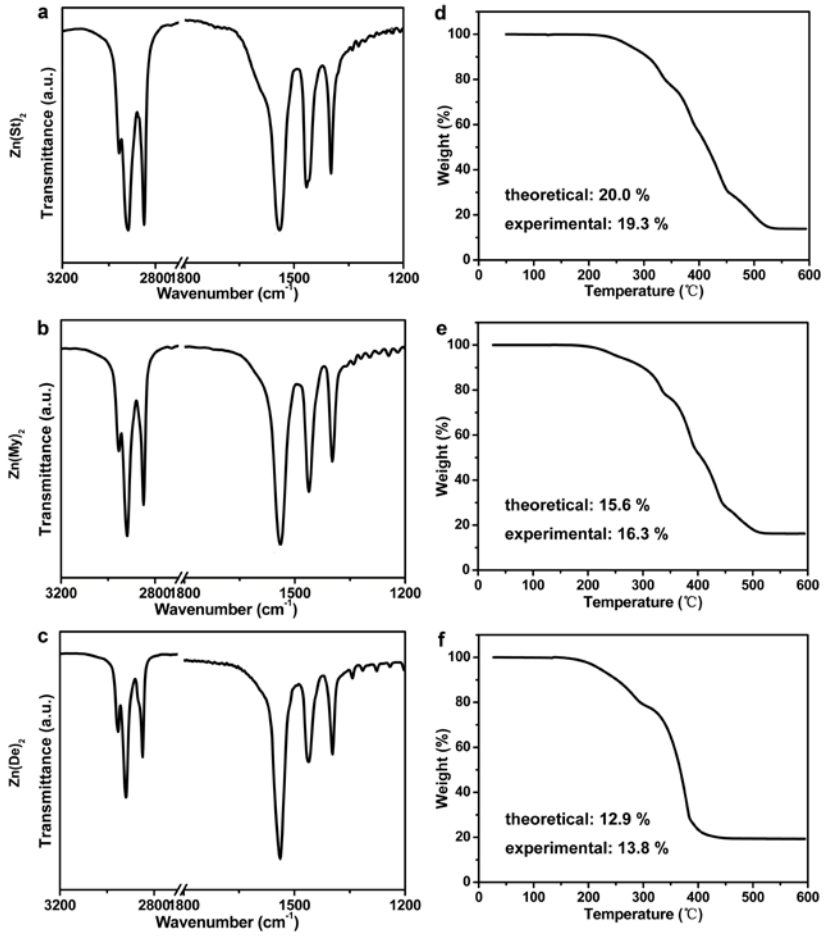

Figure S1. (a) - (c) FTIR spectra for $Zn(St)_2$, $Zn(My)_2$ and $Zn(De)_2$, respectively. The measurements were carried out at room temperature. (d) - (f) TGA profiles for $Zn(St)_2$, $Zn(My)_2$ and $Zn(De)_2$, respectively.

3. Measuring the ester concentrations by FTIR

We used a method to measure the concentrations of ester by taking the advantage of the fact that ester, the by-product of the alcoholysis reaction is readily probed by FTIR. The concentrations of ester were determined by following the Lambert–Beer law. The C=C vibration band at 1641 cm^{-1} from ODE (the solvent) was found to be a good reference for quantitative calculations.

One prerequisite of applying Lambert–Beer law to calculate the concentration of a substance is that the absorbance of all peaks in the FTIR spectra should be in the dynamic range of the instrument. In our experimental procedures, the volume of the aliquots taken out of the reaction flask by microsyringes at different time intervals was fixed to be 0.3 μL. Prior to the solidification of the reaction mixture, the aliquots were spread onto CaF_2 substrates to form smooth films with even thickness. In this way, a optimum thickness of the thin films was achieved so that the absorbance peaks were reasonably strong to maximize the signal to noise ratio and did not exceed the linear range of the FTIR analyses. Each sample were measured thrice and averaged.

We applied the above sample preparation procedures to a series of solutions of methyl stearate (MSt) dissolved in ODE with known concentrations (Figure S2a). As shown in Figure S2b, the measurements produced a linear working curve with a coefficient of determination (R^2) greater than 0.9999. This result suggests that our sample preparation procedures provide excellent accuracy for the determination of concentrations of ester.

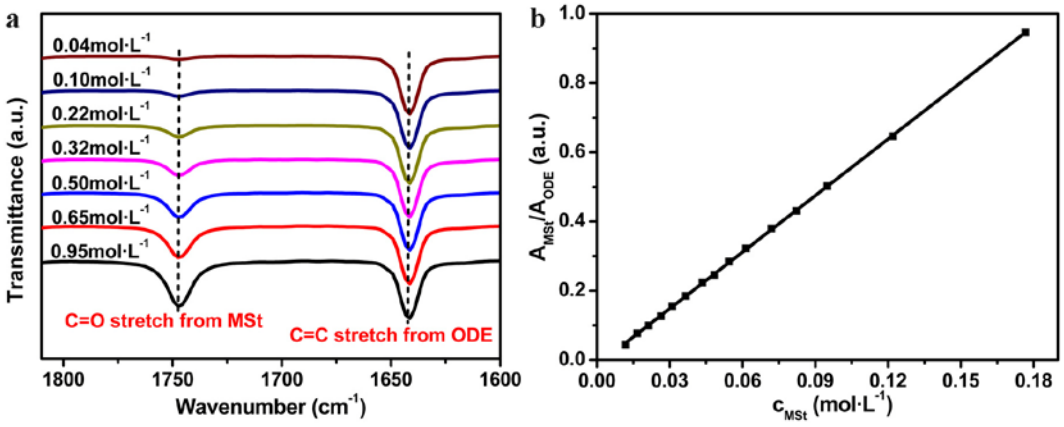

Figure S2. (a) FTIR spectra of MSt in ODE. (b) The corresponding linear working curve.

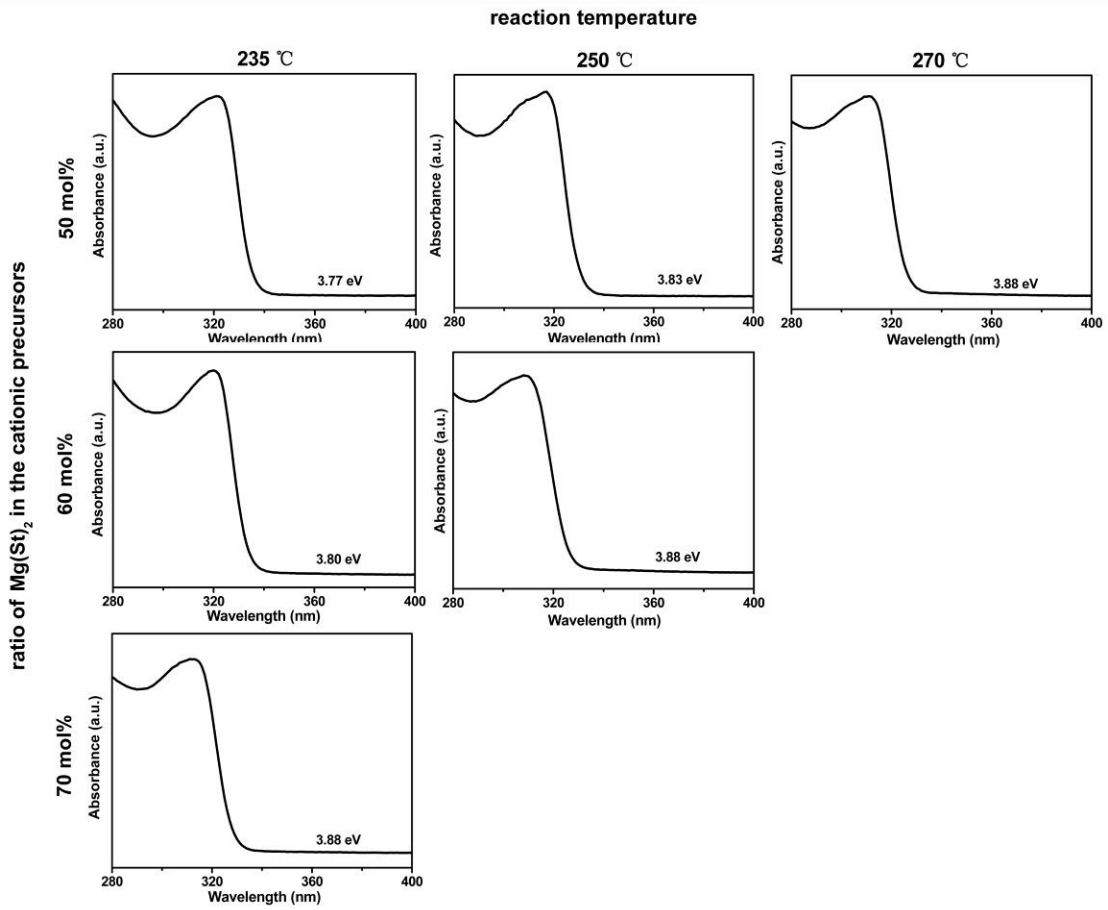

Figure S3. The UV-Vis spectra of the Mg-doped ZnO nanocrystals (corresponding to Figure 1).

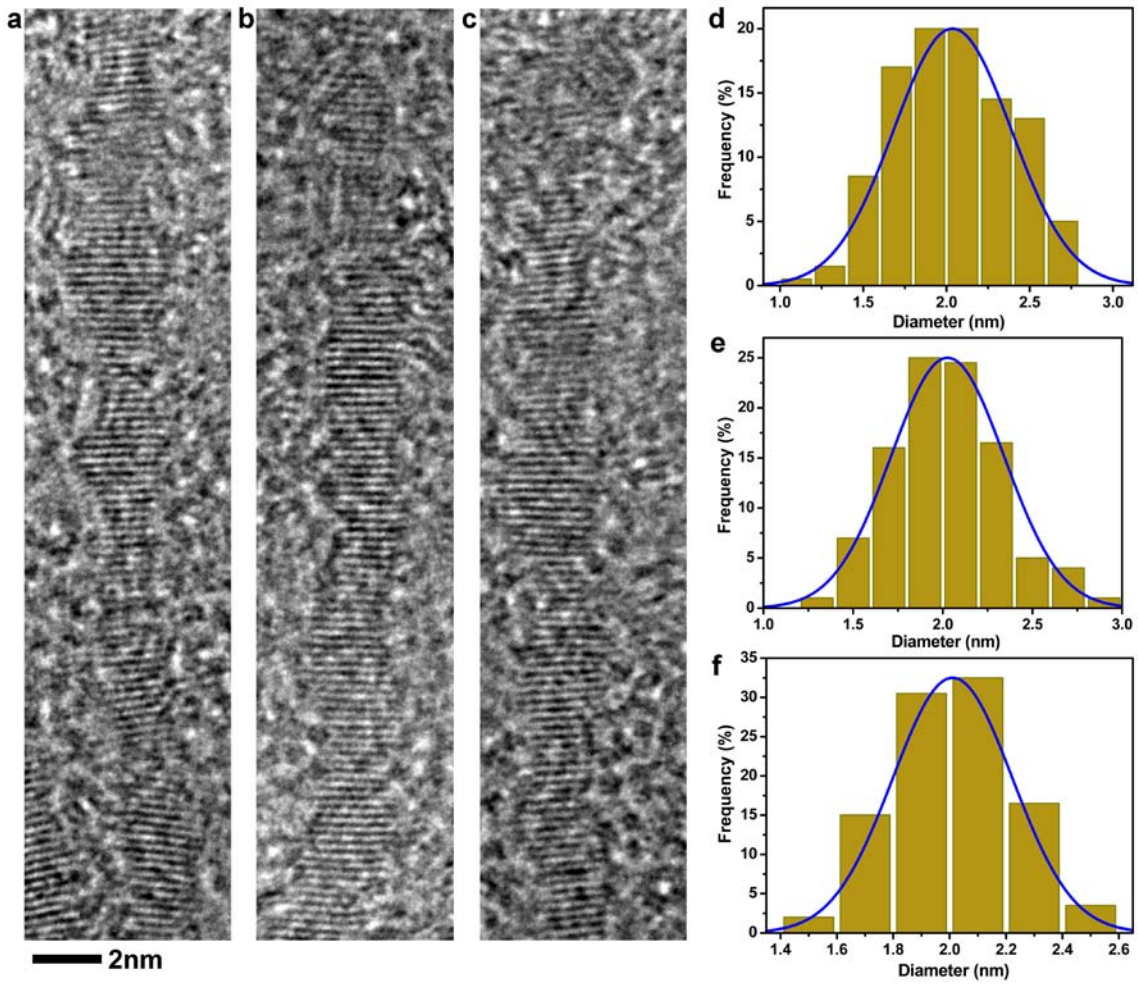

Figure S4. HRTEM analyses on the ultrathin nanowires. (a) - (c) Typical HRTEM images of the products from the reactions conducted at conditions of 235 ºC and 70 mol% of $Mg(St)_2$, 250 ºC and 60 mol% of $Mg(St)_2$, and 270 ºC and 50 mol% of $Mg(St)_2$, respectively. (d) - (f) The corresponding histograms showing the respective distributions of diameters of 200 randomly selected ultrathin nanowires.

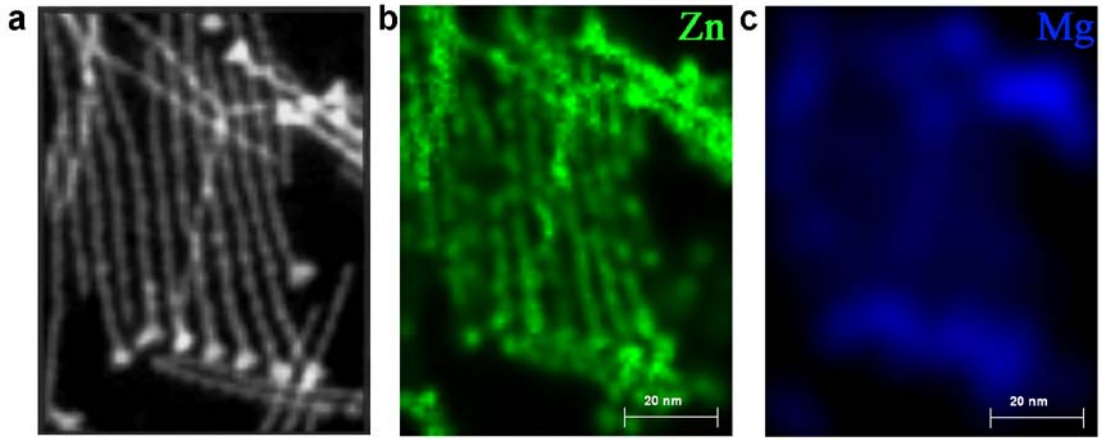

Figure S5. EDS-mapping of the Mg-doped ZnO ultrathin nanowires. (a) The HAADF image. (b) and (c) the corresponding elemental mapping for Zn and Mg, respectively.

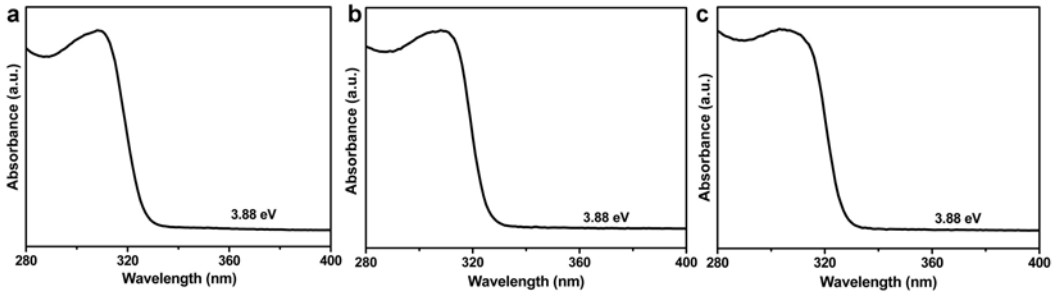

Figure S6. UV-Vis spectra of the Mg-doped ZnO ultrathin nanowires (corresponding to Figure 5).

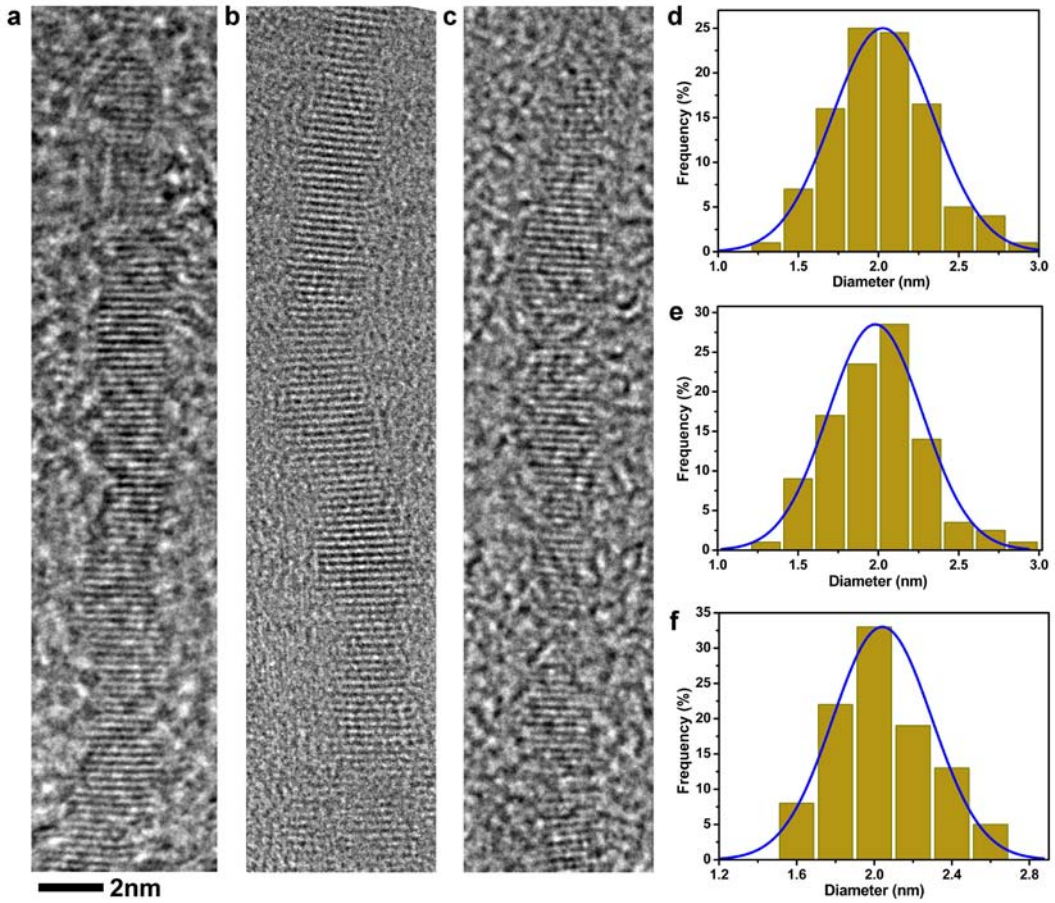

Figure S7. HRTEM analyses on the ultrathin nanowires. (a) - (c) Typical HRTEM images of the products from the reactions starting with 40 mol% of $Zn(St)_2$, 30 mol% of $Zn(My)_2$ and 35 mol% of $Zn(De)_2$, respectively (reaction temperature = 250 ºC). (d) - (f) The corresponding histograms showing the respective distributions of diameters of 200 randomly selected ultrathin nanowires.

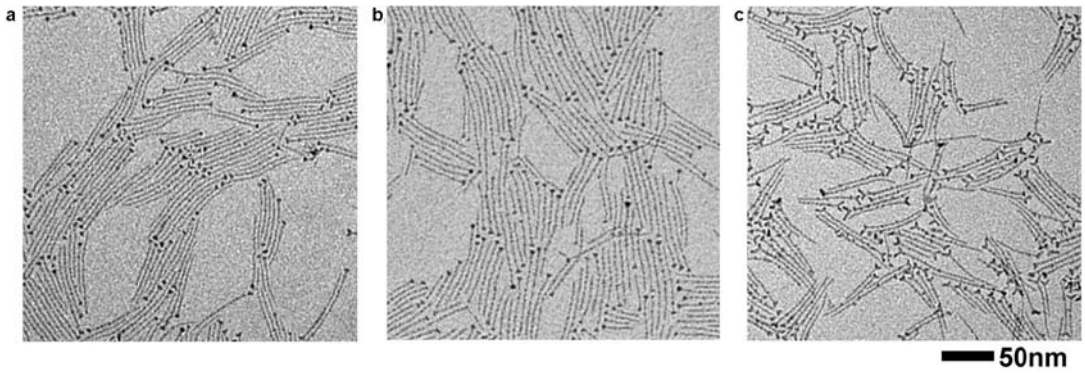

Figure S8. (a) - (c) Typical TEM images of the Mg-doped ZnO ultrathin nanowires from the reaction starting with 40 mol% of $Zn(St)_2$ and additional 0.2 mmol of HSt, 30 mol% of $Zn(My)_2$ and 0.2 mmol of HMy, and 35 mol% of $Zn(De)_2$ and 0.2 mmol of HDe, respectively. The reactions were conducted at 250 ºC.

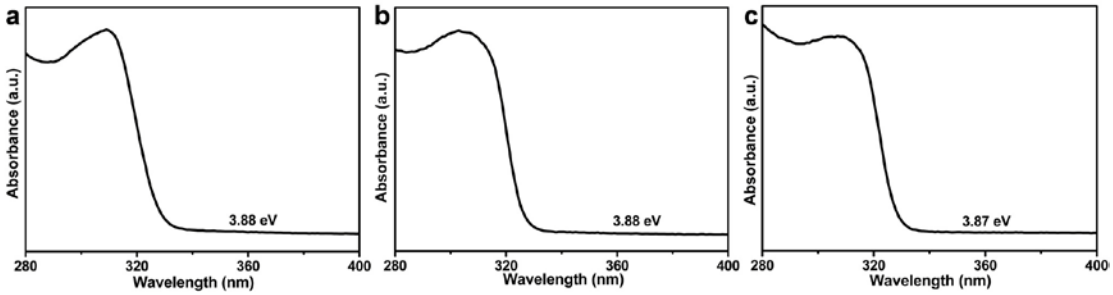

Figure S9. UV-Vis spectra of the Mg-doped ZnO ultrathin nanowires (corresponding to Figure S8).

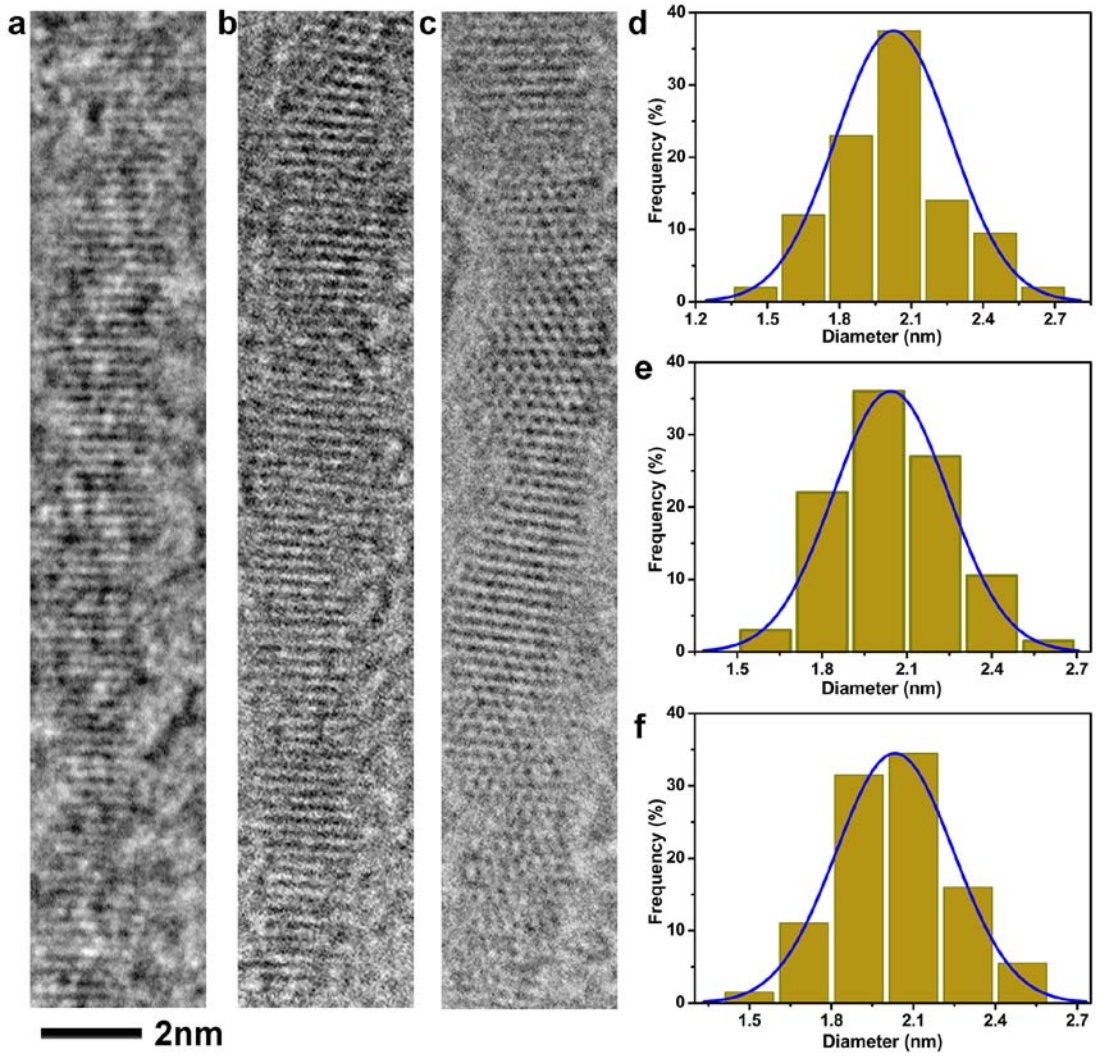

Figure S10. HRTEM analyses on the ultrathin nanowires. (a) - (c) Typical HRTEM images of the products from the reactions starting with 40 mol% of $Zn(St)_2$ and additional 0.2 mmol of HSt, 30 mol% of $Zn(My)_2$ and 0.2 mmol of HMy, and 35 mol% of $Zn(De)_2$ and 0.2 mmol of HDe, respectively (reaction temperature = 250 ºC). (d) - (f) The corresponding histograms showing the respective distributions of diameters of 200 randomly selected ultrathin nanowires.

Table S1. The properties of the Mg-doped ZnO nanocrystals synthesized with additional ligands of free fatty acids.

	40 mol% of $Zn(St)_2$ + 0.2 mmol of HSt	30 mol% of $Zn(My)_2$ + 0.2 mmol of HMy	35 mol% of $Zn(De)_2$ + 0.2 mmol of HDe
optical band gap (eV)	3.88	3.88	3.87
Mg content in NCs (at.%)	30.7	29.4	30.8
diameter (nm)	2.0 ± 0.2	2.0 ± 0.2	2.0 ± 0.2

References

1. Chen, Y., Johnson, E. & Peng, X. Formation of Monodisperse and Shape-Controlled MnO Nanocrystals in Non-Injection Synthesis: Self-Focusing via Ripening. *J. Am. Chem. Soc.* **129,** 10937-10947 (2007).

2. Wang, X. *et al.* Bandgap engineering and shape control of colloidal $Cd_xZn_{1-x}O$ nanocrystals. *Nanoscale* **5,** 6464-6468 (2013).